RESEARCH ARTICLE

annalen der physik
www.ann-phys.org

Suppressing Degradation in Quantum Batteries by Electromagnetically-Induced Transparency

*Jin-Tian Zhang, Cheng-Ge Liu, and Qing Ai**

Quantum batteries (QBs), as emerging quantum devices for energy storage and transfer, have attracted significant attention due to their potential to surpass classical batteries in charging efficiency and energy density. However, interactions between a QB and its environment result in decoherence, which significantly reduces its operational lifespan. In this work, the aging of QBs is proposed to be suppressed by introducing the electromagnetically-induced transparency (EIT). Specifically, a four-level atom is modeled as a QB with an effective two-level system enabled by the EIT, while the photons in the cavity serve as the energy charger. By comparing the energy and extractable work of the QB with and without the EIT effect, it is demonstrated that the QBs incorporating the EIT exhibit enhanced resistance to spontaneous decay as compared to their counterparts without the EIT. It is believed that the findings may provide valuable insights and shed the light on the design principles for mitigating the degradation of the QBs.

1. Introduction

Classical batteries, as electrochemical devices, store energy and provide power to electrical equipments.[1–3] Whether it is the 150 kWh battery packs in electric vehicles or the dry cells in remote controls, batteries are ubiquitous in everyday life.[4] However, with rapid technological advancements, the demand for miniaturization has become increasingly urgent in cutting-edge fields such as quantum computing,[5–7] nanotechnology,[8] and quantum communication.[9,10] This trend has driven the miniaturization of batteries. When their size is reduced to the atomic and molecular scales, quantum-mechanical effects become significant. This gave rise to the concept of quantum batteries (QBs).[4,11–13]

Quantum thermodynamics, which explores energy conversion, heat transfer, and entropy evolution in quantum systems, seeks to understand how quantum effects influence energy storage, transfer, and conversion.[14–18] One of its significant applications is the QB.[19,20] Composed of quantum bits (qubits) or quantum oscillators, the QBs offer several advantages over traditional batteries, such as significantly faster charging times, higher energy-storage efficiency, greater energy density, and increased precision and control.[21,22] These features make QBs a promising solution to energy challenges in advanced technologies. Since the concept was introduced in 2013,[21] the primary research has been focused on how to store and extract energy efficiently in QBs.[23] Currently, the QB models based on two-level systems are widely studied.[11,24–26] These batteries can interact with external agents, such as driving fields, thermal baths, or other two-level systems, to achieve charging. Despite their potential, QBs face practical challenges, one of the most notable being aging. In QBs, aging refers to the gradual decline in energy storage and extraction efficiency over time or after repeated charging-and-discharging cycles. Aging leads to reduced capacity, slower energy extraction, and even an inability to store energy effectively. In quantum systems, aging arises primarily from interactions with the external environment, e.g., thermal baths, noise, or electromagnetic fields,[24] which disrupt quantum states and lead to the loss of quantum coherence and entanglement.[12] This phenomenon, known as decoherence, significantly impacts the energy storage and extraction processes,[23] leading to performance degradation or battery aging. Decoherence is the process by which a quantum system loses its quantum-state coherence over time. Numerous methods have been proposed to suppress decoherence, such as environment engineering,[27] feedback control,[28] and Floquet engineering.[29] Inspired by these discoveries, in this paper, we explores using the electromagnetically-induced transparency (EIT) to suppress the aging of QBs.

The EIT is a quantum-optical phenomenon widely used in optics and quantum information processing.[30–32] A classical EIT system consists of a three-level system with the states $|d\rangle$, $|m\rangle$, and $|e\rangle$.[33] Here, $|d\rangle$ is the initial state, and $|m\rangle$ is the target state, and $|e\rangle$ is the intermediate state. The probe field acts between $|d\rangle$ and $|e\rangle$, while the driving field acts between $|m\rangle$ and $|e\rangle$. Under these conditions, the system can enter a coherent state, which is superposition of the bright states and dark states. The bright state is usually associated with the intermediate state $|e\rangle$, while

J.-T. Zhang, C.-G. Liu, Q. Ai
School of Physics and Astronomy
Applied Optics Beijing Area Major Laboratory
Beijing Normal University
Beijing 100875, China
E-mail: aiqing@bnu.edu.cn

J.-T. Zhang, C.-G. Liu, Q. Ai
Key Laboratory of Multiscale Spin Physics
Ministry of Education
Beijing Normal University
Beijing 100875, China

The ORCID identification number(s) for the author(s) of this article can be found under https://doi.org/10.1002/andp.202500278

DOI: 10.1002/andp.202500278

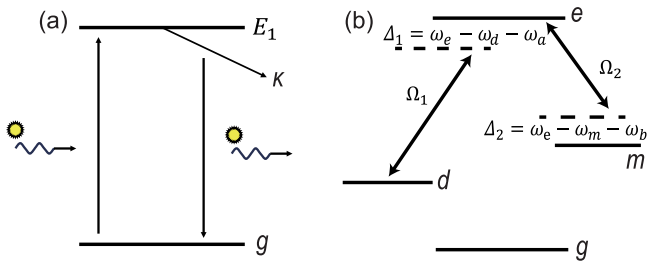

Figure 1. Schematic of a QB against degradation by the EIT. a) The QB is a two-level system including the ground state $|g\rangle$ and the dark state $|E_1\rangle$. When a photon is absorbed and the atom is excited from $|g\rangle$ to $|E_1\rangle$, the QB is charged. However, when a photon is emitted and the atom is deexcited from $|E_1\rangle$ to $|g\rangle$, the QB is discharged. b) In order to realize the dark state, a three-level configuration with two lower states $|d\rangle$ and $|m\rangle$, and the higher intermediate state $|e\rangle$ is employed. The Rabi frequencies for the transitions $|d\rangle \leftrightarrow |e\rangle$ and $|m\rangle \leftrightarrow |e\rangle$ are respectively Ω_1 and Ω_2. And Δ_1 and Δ_2 are respectively the two detunings.

the dark state is typically a superposition of $|d\rangle$ and $|m\rangle$.[34–36] Since the dark state does not involve the intermediate state $|e\rangle$, it is unaffected by the dissipation due to the coupling to the environment and is thus highly stable. This stability makes dark states less sensitive to environmental noise, and when a quantum system is in a dark state, energy loss can be avoided. The aging of QBs is largely due to decoherence caused by interactions with the external environment. This insight suggests that dark states could be employed to suppress decoherence, thereby extending the operational lifespan of QBs. Compared to other methods for suppressing decoherence, the EIT offers high stability and is relatively easy to implement, making it a viable solution to the problem of the QB aging. Refs. [37,38] also introduce dark states to suppress the dissipation in QB. Unlike them, we use a four-level atom as the QB and, by adjusting the frequency of the driving light, we can enhance the ergodicity of the QB.

This paper is structured as follows. In the next section, we introduce the QB's model. By incorporating the EIT effect into a four-level atomic system, we can effectively obtain a two-level atom with the dark state as the excited state. The detailed derivations are outlined in Appendix A. In Section 3, we consider that the four-level atom is placed in a cavity and can be charged by the photons inside the cavity. We investigate the energy and ergotropy of the QB with different numbers of atoms and photons with and without the EIT effect. Some of the detailed calculations are provided in Appendix B. We also analytically calculate the time evolution by the Wei-Norman algebra in Appendix C. Our results show that the introduction of the EIT can effectively suppress the decay of the QB's energy. Finally, in the Section 5, we summarize our main findings.

2. Model

First of all, we consider a three-level system as shown in **Figure** 1b. The Hamiltonian reads

$$H = \omega_d|d\rangle\langle d| + \omega_e|e\rangle\langle e| + \omega_m|m\rangle\langle m| + 2\Omega_1\cos\omega_a t|e\rangle\langle d| + 2\Omega_2\cos\omega_b t|e\rangle\langle m| + \text{h.c.} \quad (1)$$

where ω_d, ω_e, and ω_m are respectively the energies of the states $|d\rangle$, $|e\rangle$ and $|m\rangle$, the Rabi frequencies of the transitions $|d\rangle \leftrightarrow |e\rangle$ and $|m\rangle \leftrightarrow |e\rangle$ are respectively Ω_1 and Ω_2, ω_a, and ω_b are respectively the driving frequencies. Here, we assume $\hbar = 1$ for simplicity.

In the rotating frame with respect to $U = \exp[i(\omega_a|e\rangle\langle e| + \omega_c|m\rangle\langle m|)t]$, where $\omega_b + \omega_c = \omega_a$. Additionally, we apply the rotating-wave approximation to eliminate the rapidly oscillating, high-frequency terms. The effective Hamiltonian $H_{\text{eff}} = U^\dagger H U + iU^\dagger U$ is simplified as

$$H_{\text{eff}} = \omega_d|d\rangle\langle d| + (\omega_e + \omega_a)|e\rangle\langle e| + (\omega_m + \omega_c)|m\rangle\langle m| + \Omega_1(|e\rangle\langle d| + |d\rangle\langle e|) + \Omega_2(|e\rangle\langle m| + |m\rangle\langle e|) \quad (2)$$

On account of the dissipation on $|d\rangle$ with decay rate κ, by using the non-Hermitian Hamiltonian approach, the effectively Hamiltonian can be written in the matrix form as

$$H'_{\text{eff}} = \begin{pmatrix} \omega_d - i\kappa & \Omega_1 & 0 \\ \Omega_1 & \omega_e + \omega_a & \Omega_2 \\ 0 & \Omega_2 & \omega_m + \omega_c \end{pmatrix} \quad (3)$$

After some algebra, the effective Hamiltonian can be rewritten as

$$H'_{\text{eff}} = H_0 + I(\omega_d - i\kappa) \quad (4)$$

where

$$H_0 = \begin{pmatrix} 0 & \Omega_1 & 0 \\ \Omega_1 & \omega_1 & \Omega_2 \\ 0 & \Omega_2 & \omega_2 \end{pmatrix} \quad (5)$$

$$\omega_1 = \omega_e + \omega_a - \omega_d + i\kappa \quad (6)$$

$$\omega_2 = \omega_m + \omega_c - \omega_d + i\kappa \quad (7)$$

According to Appendix A, the Hamiltonian H_0 can be diagonalized as

$$H_0 = \sum_{j=1}^{3} x_j|E_j\rangle\langle E_j| \quad (8)$$

where the three eigen states are

$$|E_1\rangle \simeq \frac{\Omega_2}{N_1}(-\Omega_2|d\rangle + \Omega_1|m\rangle) \quad (9)$$

$$|E_2\rangle \simeq \frac{\Omega_1}{N_2}(\Omega_1|d\rangle + \Omega|e\rangle + \Omega_2|m\rangle) \quad (10)$$

$$|E_3\rangle \simeq \frac{\Omega_1}{N_3}(\Omega_1|d\rangle - \Omega|e\rangle + \Omega_2|m\rangle) \quad (11)$$

By substituting H_0 into H'_{eff}, we can obtain

$$H'_{\text{eff}} = \sum_{j=1}^{3} x'_j|E_j\rangle\langle E_j| \quad (12)$$

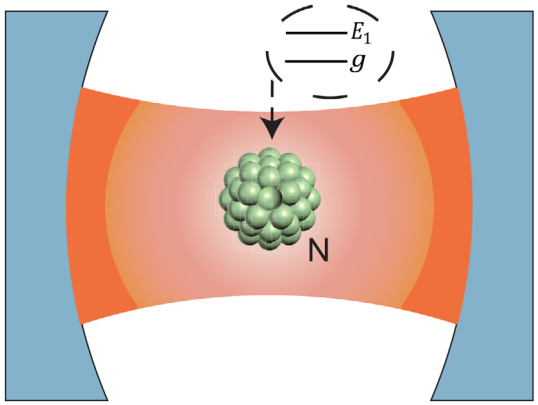

Figure 2. Schematic of a QB with a collective of atoms in a cavity. There are effectively N two-level atoms with the ground state g and the dark state E_1 located in a cavity.

where

$$x_1' = \frac{\Omega_1^2}{\Omega^2}(\omega_m + \omega_c - \omega_d) + \omega_d - i\frac{\Omega_2^2}{\Omega^2}\kappa \tag{13}$$

$$x_2' = \Omega + \frac{\omega_e + \omega_a}{2} + \frac{\omega_m + \omega_c}{2\Omega^2}\Omega_2^2 + \frac{\Omega_1^2\omega_d}{2\Omega^2} - \frac{i\Omega_1^2\kappa}{2\Omega^2} \tag{14}$$

$$x_3' = -\Omega + \frac{\omega_e + \omega_a}{2} + \frac{\omega_m - \omega_c}{2\Omega^2}\Omega_2^2 + \frac{\Omega_1^2\omega_d}{2\Omega^2} - \frac{i\Omega_1^2\kappa}{2\Omega^2} \tag{15}$$

The imaginary parts of x_j's represent the relaxation rate of the system. Compared to the original decay rate κ, the current decay rates are respectively $\Omega_2^2\kappa/\Omega^2$ for $|E_1\rangle$ and $\Omega_1^2\kappa/2\Omega^2$ for $|E_2\rangle$ and $|E_3\rangle$. If we tune $\Omega_1 \gg \Omega_2$, we have $\Omega_2^2\kappa/\Omega^2 \simeq 0$ and $\Omega_1^2\kappa/2\Omega^2 \simeq \kappa/2$. In other words, $|E_1\rangle$ is the dark state because its relaxation has been significantly suppressed, while $|E_2\rangle$ and $|E_3\rangle$ are the two bright states. In this regards, we utilize the dark state and the ground state to establish a QB against the aging.

3. Numerical Simulation and Discussions

Based on the above discussions, as shown in **Figure 2**, when $N = 1$, we consider a two-level atom with the ground state $|g\rangle$ and the dark state $|E_1\rangle$ in a cavity. The total Hamiltonian is

$$H = x_1'|E_1\rangle\langle E_1| + \omega a^+ a + Ja^+\sigma^- + Ja\sigma^+ \tag{16}$$

where J is the coupling constant between the atom and the cavity, $a^\dagger$ (a) is the creation (annihilation) operator of the cavity mode with frequency ω. $\sigma^+ = |E_1\rangle\langle g| = (\sigma^-)^\dagger$ is the atomic raising operator.

In the subspace spanned by the two bases $|n\rangle|E_1\rangle$ and $|n+1\rangle|g\rangle$, the total Hamiltonian can be rewritten in the matrix form as

$$H = \begin{pmatrix} x_1' - \frac{\omega}{2} & J \\ J & \frac{\omega}{2} \end{pmatrix} + \left(n + \frac{1}{2}\right)\omega \tag{17}$$

where the two eigen energies are

$$\lambda_n^\pm = \frac{1}{2}\left(x_1' \pm \sqrt{4J^2 + (\omega - x_1')^2}\right) + \left(n + \frac{1}{2}\right)\omega \tag{18}$$

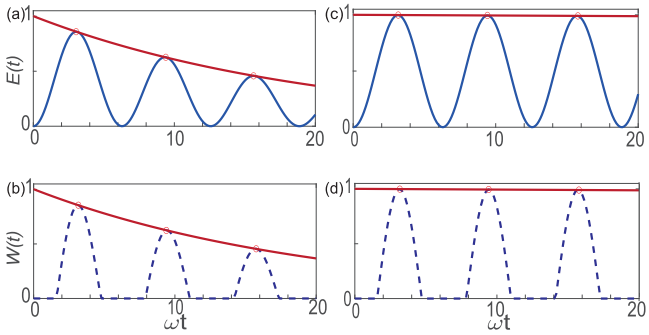

Figure 3. The effects of the EIT on the system's energy $E(t)$ and ergodicity $W(t)$ with $N = 1$ atom and $n = 1$ photon. a) $E(t)$ and b) $W(t)$ without the EIT, c) $E(t)$ and (d) $W(t)$ with the EIT. The parameters are $\omega = 1, J = 0.5\omega$, $\omega_m = 0.5\omega$, $\omega_e = \omega$, $\omega_d = 0.25\omega$, $\Omega_1 = 50\omega$, $\Omega_2 = 5\omega$, $\kappa = 0.05\omega$. The red solid line denotes the envelope which is numerically fitted by an exponential decay.

and the two eigen states are

$$|\psi_n^+\rangle = \frac{1}{N_n^+}\begin{pmatrix} J \\ \lambda_n^+ - x_1' - n\omega \end{pmatrix} \tag{19}$$

$$|\psi_n^-\rangle = \frac{1}{N_n^-}\begin{pmatrix} J \\ \lambda_n^- - x_1' - n\omega \end{pmatrix} \tag{20}$$

$$N_n^\pm = \sqrt{\left(x_1' + n\omega - \lambda_n^\pm\right)^2 + J^2} \tag{21}$$

are the normalization constants.

Assuming the initial state $|n\rangle|E_1\rangle$, the time evolution of the system can be given as

$$|\psi(t)\rangle = \sum_{\alpha=\pm}\frac{\lambda_n^\alpha - x_1' - n\omega}{N_n^\alpha}e^{-i\lambda_n^\alpha t}|\psi_n^\alpha\rangle \tag{22}$$

In the QB, the total Hamiltonian can be divided into three parts as $H = H_A + H_B + H_I$, where H_A is the Hamiltonian of the charger, H_B is the Hamiltonian of the QB, and H_I is the interaction Hamiltonian between them. The ergotropy is equal to ref. [23]

$$W(t) = \mathrm{Tr}[\rho_B(t)H_B] - \mathrm{Tr}[\tilde{\rho}_B(t)H_B] \tag{23}$$

where the energy of the QB is $E(t) = \mathrm{Tr}[\rho_B(t)H_B]$, $E_0(t) = \mathrm{Tr}[\tilde{\rho}_B(t)H_B]$ is the energy of the passive state. Here, $\rho_B(t) = \sum_n r_n|r_n\rangle\langle r_n|$ is the reduced density matrix of the QB, $\tilde{\rho}_B(t) \equiv \sum_n r_n|\epsilon_n\rangle\langle\epsilon_n|$, $H_B = \sum_n \epsilon_n|\epsilon_n\rangle\langle\epsilon_n|$, $r_1 \geq r_2 \geq \cdots$, and $\epsilon_1 \leq \epsilon_2 \leq \cdots$. When $W(t) = 0$, the system is in a passive state, which implies that we can not extract any energy from the system. **Figure 3** shows the system's ergodicity over time. When the EIT is absent, we can see that $W(t)$ declines exponentially with respect to the time. However, when the EIT is introduced, $W(t)$ generally oscillate with time. If we fit the envelope of $W(t)$ by an exponential function, we could obtain $\exp(-5.01 \times 10^{-2}\omega t)$ and $\exp(-6.76 \times 10^{-4}\omega t)$ for the two cases respectively. In other words, the decay of the ergodicity is reduced by two orders of magnitude due to the presence of the EIT.

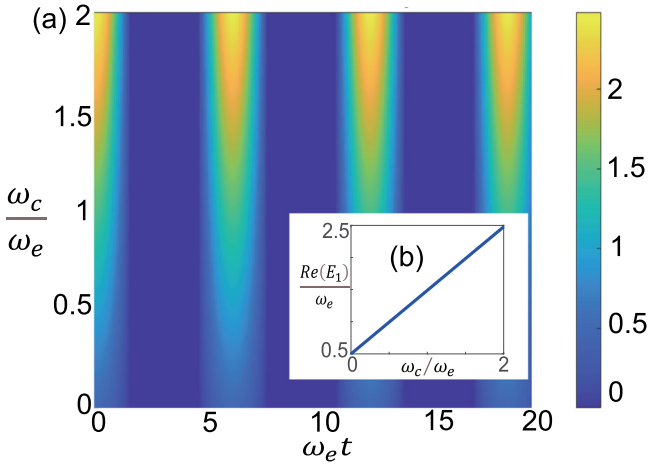

Figure 4. a) The effects of the EIT on the system's ergodicity as a function of the dimensionless time $\omega_e t$ and ω_c/ω_e and b) the inset shows the relation between E_1 and ω_c/ω_e. The parameters are $\omega_e = 1\ \Omega_1 = 50\omega_e$, $\Omega_2 = 5\omega_e$, $\Omega = \sqrt{\Omega_1^2 + \Omega_2^2}$, $\omega_d = 0.25\omega_e$, $\omega_m = 0.5\omega_e$, $\omega_a = x\omega_e$, $\omega_b = 0.5\omega_e$, $\omega_c = \omega_a - \omega_b$, $\kappa = 0.05\omega_e$, $\omega = E_1$, and $J = 0.5\omega_e$.

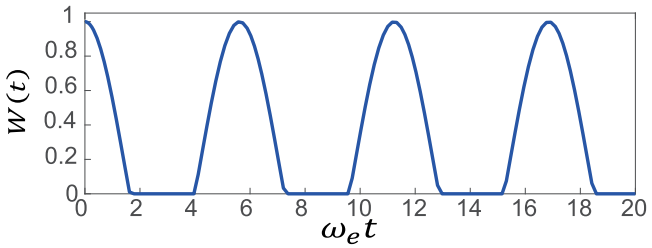

Figure 5. Time evolution of the ergodicity $W(t)$ as a function of the dimensionless time $\omega_e t$. The parameters are $\omega_e = 1\ E_1 = \omega_e, J = 0.5\omega_e$, and $\omega = 0.5\omega_e$.

After the EIT is introduced in QB, the dissipation can not only be reduced, but the ergodicity can also be enhanced by tuning the parameters. We construct a dark state E_1 as the effective excited state by coupling the states d and m. According to Equation (9), also shown in **Figure** 4b, the energy of the constructed excited state E_1 is positively correlated with ω_c. Hence, by adjusting ω_c, the energy of the excited state can be increased.

In Figure 4, since $\omega_c = \omega_a - \omega_b$, we fix ω_b and vary ω_a to tune ω_c. We found that the larger ω_c is, the greater the ergodicity becomes. By contrast, if we use the lower-dissipation state e as the excited state, thereby forming a conventional two-level QB, cf. **Figure** 5, the maximum ergodicity only reaches 1. Compared to the traditional two-level QB, our system achieves a substantial improvement in ergodicity with the introduction of only two auxiliary states, while reducing the system's dissipation with the help of the EIT. As a concrete example, we propose constructing the QB using the $5S_{1/2}$, $5P_{1/2}$, $5P_{3/2}$, and $6S_{1/2}$ levels of rubidium atoms.[39]

Figure 6 shows the quantum dynamical evolution of the system. Initially, the system is in $|0\rangle|E_1\rangle$. In the absence of the EIT, the system decay significantly, as the oscillatory behavior diminishes rapidly, leading to a noticeable reduction in the amplitude of the probability curves. However, when the EIT is introduced, the two probabilities oscillate with the same amplitude and frequency. Notably, the oscillations occur almost without any observable decay. This suggests that the system's energy remains largely unchanged. Similarly, we can also fit the envelope of the probabilities by an exponential function. Thus, we obtain $\exp(-5.00 \times 10^{-2}\omega t)$ and $\exp(-5.38 \times 10^{-4}\omega t)$ for the two cases respectively, which are consistent with those for the ergodicity in Figure 3. These suggest that due to the EIT, the dissipation has been significantly suppressed and thus the ergodicity is improved.

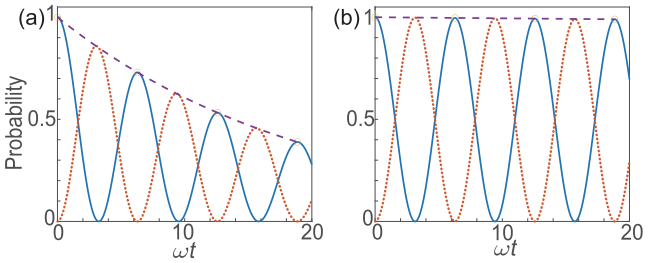

Figure 6. The probabilities of the two states $|0\rangle|E_1\rangle$ (blue solid line) and $|1\rangle|g\rangle$ (red dotted line) over time a) without the EIT and b) with the EIT. The parameters are the same as Figure 3. The purple dashed line denotes the numerical fitting by an exponential function.

Furthermore, we consider a cavity with N quasi-two-level atoms and a single photon. The Hamiltonian reads

$$H = \omega a^\dagger a + \sum_{j=1}^{N} \left(x_1' \sigma_j^+ \sigma_j^- + Ja\sigma_j^+ + \text{h.c.} \right) \tag{24}$$

where $\sigma_j^+ = |E_1\rangle_{jj}\langle g| = (\sigma_j^-)^\dagger$ is the raising operator of jth atom.

At time t, the total system is in the state

$$|\psi(t)\rangle = \left[c_0(t)a^\dagger + \sum_{i=1}^{n} c_i(t)\sigma_i^+ \right] |G\rangle|0\rangle \tag{25}$$

where $|G\rangle = |g\rangle_1 \otimes |g\rangle_2 \otimes \cdots \otimes |g\rangle_n$ is the state for all atoms being in the ground states. By substituting Equation (25) into the Schrödinger equation, we can obtain

$$i\dot{c_0}(t) = \omega c_0(t) + J \sum_{j=1}^{n} c_j(t) \tag{26}$$

$$i\dot{c_j}(t) = x_1' c_j(t) + J c_0(t) \tag{27}$$

where $c_0(0) = 1$ and $c_j(0) = 0$ are the initial conditions of this system. By performing the Laplace transform $\mathcal{L}\{df(t)/dt\} = s\tilde{f}(s) - f(0)$ on Equations (26) and (27), we can obtain

$$\tilde{c}_0(s) = \frac{i(is - x_1')}{(is - \omega_0)(is - x_1') - nJ^2} \tag{28}$$

$$\tilde{c}_j(s) = \frac{iJ}{(is - \omega_0)(is - x_1') - nJ^2} \tag{29}$$

After some algebra, $\tilde{c}_0(s)$ and $\tilde{c}_j(s)$ can be rewritten as

$$\tilde{c}_0(s) = \frac{i(is - x_1')}{(s - s_+)(s - s_-)} = \frac{A_+}{s - s_+} + \frac{A_-}{s - s_-} \tag{30}$$

$$\tilde{c}_j(s) = \frac{iJ}{(s - s_+)(s - s_-)} = \frac{B_+}{s - s_+} + \frac{B_-}{s - s_-} \tag{31}$$

where

$$s_\pm = -i\frac{(\omega_0 + x_1') \pm \sqrt{(\omega_0 - x_1')^2 - nJ^2}}{2} \tag{32}$$

$$A_\pm = \pm\frac{i(is_\pm - x_1')}{s_+ - s_-} \tag{33}$$

$$B_\pm = \pm\frac{iJ}{s_+ - s_-} \tag{34}$$

By using the inverse Laplace transform, we can obtain

$$c_0(t) = A_+ e^{s_+ t} + A_- e^{s_- t} \tag{35}$$

$$c_j(t) = B_+ e^{s_+ t} + B_- e^{s_- t} \tag{36}$$

By partially tracing the degrees of freedom of the cavity, the reduced density matrix of the atoms reads

$$\rho_B(t) = |c_0|^2 |G\rangle\langle g| + \sum_{j=1}^{n} |c_j|^2 \sigma_j^+ |G\rangle\langle g|\sigma_j^- + \sum_{j=1}^{n}\sum_{k\neq j} c_j c_k^* \sigma_j^+ |G\rangle\langle g|\sigma_k^- \tag{37}$$

As a result, the energy of the system $E_B^N(t) = \mathrm{Tr}[\rho_B(t) H_B]$ is equal to $x_1' \sum_{j=1}^{n} |c_j(t)|^2$.

Figure 7 shows the time evolution of the energy of the system. Initially, the system is in an excited state. The energy of the system decays significantly when the EIT is absent. However, when the EIT is introduced, the energy decay is markedly suppressed. After fitting the envelopes of the probabilities by an exponential function, we can obtain $\exp(-5.03 \times 10^{-2}\omega t)$ and $\exp(-5.78 \times 10^{-4}\omega t)$ for the two cases, respectively. Here, we extend the single-atom system to a multi-atom system. The results indicate that the EIT continues to suppresses the decay of system energy, prolonging the lifetime of QB.

In the above calculations, we obtain the analytical solution by the Laplace transform. Alternatively, hereafter we will obtain the analytical solution by the Wei-Norman algebra. By introducing the collective operators

$$J_z = \frac{1}{2}\sum_j \sigma_j^z \tag{38}$$

$$J_+ = J_-^\dagger = \sum_j \sigma_j^+ \tag{39}$$

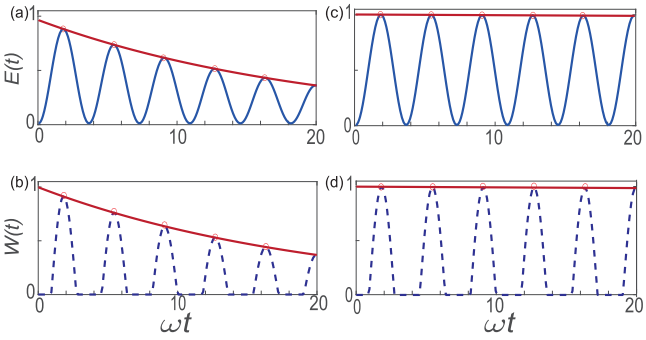

Figure 7. The effects of the EIT on the system's energy $E(t)$ and ergodicity $W(t)$ with $N = 3$ atoms and $n = 1$ photon. a) $E(t)$ and b) $W(t)$ without the EIT, c) $E(t)$ and d) $E(t)$ with the EIT. The parameters are $\omega = 1$, $J = 0.5\omega$, $\omega_m = 0.5\omega$, $\omega_e = \omega$, $\omega_d = 0.25\omega$, $\Omega_1 = 50\omega$, $\Omega_2 = 5\omega$, and $\kappa = 0.05\omega$. The red solid line denotes the envelope which is numerically fitted by an exponential decay.

and using the Holstein-Primakoff transformation [40]

$$b^\dagger b = J_z + \frac{N}{2} \tag{40}$$

$$J_+ = b^\dagger\sqrt{N}\sqrt{1 - \frac{b^\dagger b}{N}} \simeq b^\dagger\sqrt{N} \tag{41}$$

the Hamiltonian can be rewritten as

$$H \simeq \omega a^\dagger a + x_1' b^\dagger b + J_N(ab^\dagger + a^\dagger b) \tag{42}$$

where the interaction $J_N = J\sqrt{N}$ between the cavity mode and the collective excitation of the atoms has been enhanced by a factor $\sqrt{N}$.

Assuming that the initial state of the cavity is in the coherent state, and all of the two-level atoms are initially in the ground state, i.e., $|\Psi(0)\rangle = |\sqrt{N}\rangle_A \otimes |0\rangle_B$. According to Appendix C, the state of the total system at time t reads

$$|\Psi(t)\rangle = |\sqrt{N}\cos(J_N t)\rangle_A \otimes |-i\sqrt{N}\sin(J_N t)\rangle_B \tag{43}$$

When there are *three* atoms and *three* photons in the cavity, in **Figure 8**, we find that the maximum of the total energy is increased as compared to the case with *three* atoms and *one* photon because more atoms can be excited by photons. In addition, by fitting the envelopes with an exponential function, we obtain a decay rate with $-1.91 \times 10^{-3}\omega$ ($-1.94 \times 10^{-1}\omega$) for the case with (without) the EIT. When the EIT is absent, both the system's energy and ergotropy exhibit a rapid decay. However, when the EIT is introduced, both the energy and ergotropy curves exhibit pronounced oscillatory behavior. This indicates that the EIT does not only slow down the energy loss but also preserves the oscillatory characteristics of the system.

When two photons and $N_a = 2$ atoms in the cavity, on account of the dipole–dipole interaction,[44] the Hamiltonian becomes

$$H = \omega\, a^\dagger a + H_B + J\sum_{i=1}^{N_a}\left(a\,\sigma_i^+ + a^\dagger\,\sigma_i^-\right) \tag{44}$$

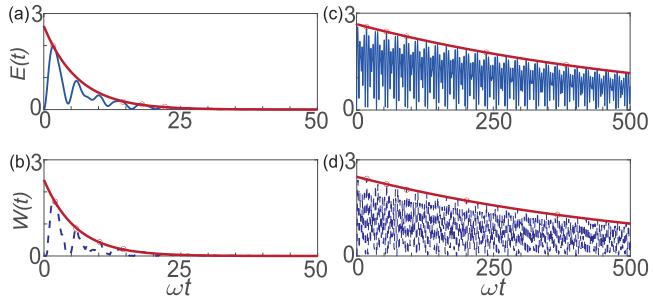

Figure 8. The effects of the EIT on the system's energy $E(t)$ and ergodicity $W(t)$ with $N = 3$ atoms and $n = 3$ photons. a) $E(t)$ and b) $W(t)$ without the EIT, c) $E(t)$ and d) $W(t)$ with the EIT. The parameters are $\omega = 1, J = 0.5\omega$, $\omega_m = 0.5\omega$, $\omega_e = \omega$, $\omega_d = 0.25\omega$, $\Omega_1 = 50\omega$, $\Omega_2 = 5\omega$, $\kappa = 0.05\omega$. The red solid line denotes the enelope which is numerically fitted by an exponential decay.

where the Hamiltonian of the QB reads

$$H_B = x_1' \sum_{i=1}^{N_a} \sigma_i^+ \sigma_i^- + \sum_{i\neq j}^{N_a} V\left(\sigma_i^+ \sigma_j^- + \sigma_i^- \sigma_j^+\right) \tag{45}$$

Its eigenvalues and eigenstates are respectively

$$E_G = 0, \qquad |G\rangle = |gg\rangle \tag{46}$$

$$E_q = E_1 + V, \qquad |q\rangle = \tfrac{1}{\sqrt{2}}\left(|eg\rangle + |ge\rangle\right) \tag{47}$$

$$E_p = E_1 - V, \qquad |p\rangle = \tfrac{1}{\sqrt{2}}\left(|eg\rangle - |ge\rangle\right) \tag{48}$$

$$E_E = 2E_1, \qquad |E\rangle = |ee\rangle \tag{49}$$

here, $|q\rangle$ is the symmetric state and $|p\rangle$ the antisymmetric state. Since

$$\sum_{i=1}^{2} \sigma_i^+ |G\rangle = |eg\rangle + |ge\rangle = \sqrt{2}\,|q\rangle \tag{50}$$

$$\sum_{i=1}^{2} \sigma_i^+ |q\rangle = \tfrac{1}{\sqrt{2}}(|ee\rangle + |ee\rangle) = \sqrt{2}\,|E\rangle \tag{51}$$

$$\sum_{i=1}^{2} \sigma_i^+ |p\rangle = \tfrac{1}{\sqrt{2}}(|ee\rangle - |ee\rangle) = 0 \tag{52}$$

$$\sum_{i=1}^{2} \sigma_i^+ |E\rangle = 0 \tag{53}$$

in the eigenbasis of H_B, the total Hamiltonian can be rewritten as

$$H = \omega\, a^\dagger a + H_B + \sqrt{2}\,Ja(\,|q\rangle\langle G| + \,|E\rangle\langle q|) + \text{h.c.} \tag{54}$$

Originally, the system include two excitation pathways, $|gg\rangle \leftrightarrow |eg\rangle \leftrightarrow |ee\rangle$ and $|gg\rangle \leftrightarrow |ge\rangle \leftrightarrow |ee\rangle$. However, after including the dipole–dipole interaction, only one pathway remains, i.e., $|gg\rangle \leftrightarrow |q\rangle \leftrightarrow |ee\rangle$, indicating a reduction in available transition channels.

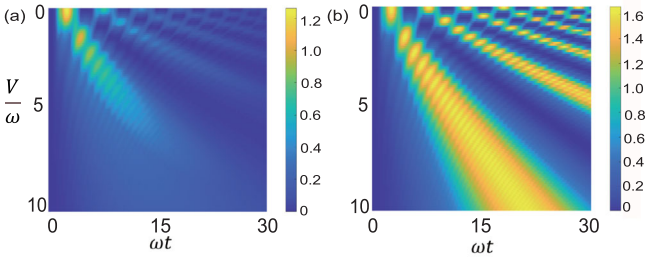

Figure 9. Ergodicity as a function of the dipole-dipole interaction V between the atoms and the time t for two atoms and two photons in the cavity (a) without the EIT and (b) with the EIT. The parameters are $\omega = 1$, $J = 0.5\omega$, $\omega_m = 0.5\omega$, $\omega_e = \omega$, $\omega_d = 0.25\omega$, $\Omega_1 = 50\omega$, $\Omega_2 = 5\omega$, and $\kappa = 0.05\omega$.

Furthermore, we consider the effect of the dipole–dipole coupling on the ergodicity. The QB Hamiltonian can be written in the basis $\{|G\rangle, |p\rangle, |q\rangle, |E\rangle\}$ as

$$H_B = \begin{pmatrix} 0 & 0 & 0 & 0 \\ 0 & E_1 - V & 0 & 0 \\ 0 & 0 & E_1 + V & 0 \\ 0 & 0 & 0 & 2E_1 \end{pmatrix} \tag{55}$$

And the density matrix is $\rho_B = \sum_{\alpha=G,q,p,E} P_\alpha |\alpha\rangle\langle\alpha|$. Ordering its eigenvalues $P_{\alpha'}$ in descending order yields $\widetilde{\rho}_B = \sum_{\alpha'=1}^{4} P_{\alpha'} |\alpha'\rangle\langle\alpha'|$, which will be used in evaluating the ergodicity.

When there are two atoms and two photons, the dynamics of the ergodicity is shown in **Figure 9**. When the system does not include the EIT, the atoms exhibit large dissipation, causing the energy of the QB to decay more rapidly over time, as shown in Figure 9a. However, one can see that when the EIT is introduced, the decay of the maximum ergodicity of the QB will be significantly slowed down. Interestingly, the first time for the ergodicity to reach the maximum will be delayed and its duration will be prolonged as V increases.

Furthermore, we consider there are $N_a = 3$ atoms in the cavity. Since the antisymmetric states do not couple to the cavity field, we restrict ourselves to the four fully-symmetric eigenstates. They and their eigenvalues are listed as

$$E_0 = 0,\ |D_{3,0}\rangle = |ggg\rangle \tag{56}$$

$$E_1 = E_1 + 2V,\ |D_{3,1}\rangle = \frac{1}{\sqrt{3}}\left(|egg\rangle + |geg\rangle + |gge\rangle\right) \tag{57}$$

$$E_2 = 2E_1 + 2V,\ |D_{3,2}\rangle = \frac{1}{\sqrt{3}}\left(|eeg\rangle + |ege\rangle + |gee\rangle\right) \tag{58}$$

$$E_3 = 3E_1,\ |D_{3,3}\rangle = |eee\rangle \tag{59}$$

Expanding the full Hamiltonian in the basis $\{|D_{3,k}\rangle\}$, one finds

$$H = \omega a^\dagger a + \sum_{k=0}^{3} E_k\, |D_{3,k}\rangle\langle D_{3,k}| \tag{60}$$

$$+ J\Big(\sqrt{3}\,a\,|D_{3,1}\rangle\langle D_{3,0}| + 2\,a\,|D_{3,2}\rangle\langle D_{3,1}| \tag{61}$$

$$+ \sqrt{3}\,a\,|D_{3,3}\rangle\langle D_{3,2}|\Big) + \text{h.c.} \tag{62}$$

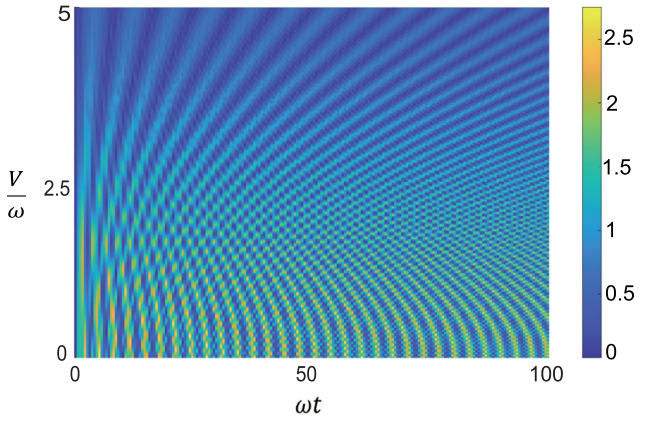

Figure 10. Ergodicity as a function of V and t for a system with 3 atoms and 3 photons in the cavity with the EIT. The parameters are $\omega = 1$, $J = 0.5\omega$, $\omega_m = 0.5\omega$, $\omega_e = \omega$, $\omega_d = 0.25\omega$, $\Omega_1 = 50\omega$, $\Omega_2 = 5\omega$, and $\kappa = 0.05\omega$.

Unlike the case of two atoms in the cavity, when there are three atoms in the cavity, the level spacings between the two neighboring eigenstates are respectively $E_1 - E_0 = E_1 + 2V$, $E_2 - E_1 = E_1$, $E_3 - E_2 = E_1 - 2V$. When the photon energy equals E_1, the detunings are $-2V$, 0, and $2V$. Because the correspond oscillation frequencies are not the same, it leads to a more-complex situation. In **Figure 10**, we find that as V increases, the maximum ergodicity gradually decreases. Since the value of V decreases rapidly with increasing interatomic distance, in practice we can reduce the influence of dipole-dipole interactions by increasing the distances between atoms.

When an electromagnetic drive with frequency ω_L and Rabi frequency Ω is applied, and the cavity contains two photons, the total Hamiltonian with $N_a = 2$ atoms becomes

$$H_{\text{tot}} = x_1' \sum_{i=1}^{N_a} \sigma_i^+ \sigma_i^- + \sum_{i \neq j} V\left(\sigma_i^+ \sigma_j^- + \sigma_i^- \sigma_j^+\right) + H_{\text{d}} \tag{63}$$

where

$$H_{\text{d}} = \sum_{i=1}^{N_a} \frac{\Omega}{2}\left(\sigma_i^+ e^{-i\omega_L t} + \sigma_i^- e^{+i\omega_L t}\right) \tag{64}$$

Transforming into the rotating frame defined by $U(t) = \exp\left(-i\,\omega_L \sum_i \sigma_i^+ \sigma_i^-\, t\right)$ and applying the rotating–wave approximation yields

$$H_{\text{eff}} = \sum_{i=1}^{N_a} \left(\Delta_L \sigma_i^+ \sigma_i^- + \frac{\Omega}{2}\sigma_i^+\right) + \sum_{i \neq j}^{N_a} V \sigma_i^+ \sigma_j^- + \text{h.c.} \tag{65}$$

with $\Delta_L = E_1 - \omega_L$. Focusing on the QB, we have

$$H_B = \Delta_L\, \sigma^+ \sigma^- + \frac{\Omega}{2}(\sigma^+ + \sigma^-) \tag{66}$$

whose eigenvalues are $E_\pm = \left(\Delta_L \pm \sqrt{\Delta_L^2 + \Omega^2}\right)/2$. For $\Delta_L \gg \Omega$, since $\sqrt{\Delta_L^2 + \Omega^2} \approx \Delta_L + (\Omega^2/2\Delta_L)$, we have

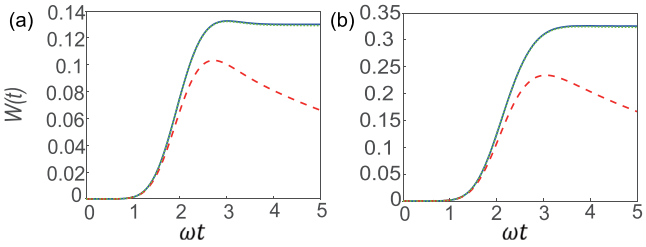

Figure 11. The time evolution of the ergodicity with a) $V = 2$ and b) $V = 1$. The blue solid line represents the QB without dissipation, the green dotted line represents the QB with the EIT, and the red dashed line represents the QB without the EIT. The parameters are $\omega = 1$, $J = 0.5\omega$, $\omega_m = 0.5\omega$, $\omega_e = \omega$, $\omega_d = 0.25\omega$, $\Omega_1 = 50\omega$, $\Omega_2 = 5\omega$, $t_c = 1.6/\omega$, $\sigma = 0.8/\omega$ and $\kappa = 0.05\omega$. Notice that the blue solid line almost overlaps with the green dotted line.

$$E_+ = \Delta_L + \frac{\Omega^2}{4\Delta_L} \tag{67}$$

$$E_- = -\frac{\Omega^2}{4\Delta_L} \tag{68}$$

In other words, the excited level is shifted up by $\frac{\Omega^2}{4\Delta_L}$ while the ground level is shifted down by the same amount. Consequently, the total Hamiltonian can be recast as

$$H_{\text{tot}} = \left(E_1 + \frac{\Omega^2}{2\Delta_L}\right) \sum_{i=1}^{N_a} \sigma_i^+ \sigma_i^- + \sum_{i \neq j} V \sigma_i^+ \sigma_j^- + \text{h.c.} \tag{69}$$

We further consider a Gaussian pulse with $\Omega(t) = \Omega_0 \exp\left[-(t - t_c)^2/2\sigma^2\right]$ is used to excite the atoms, where t_c is the center of the pulse, σ is the width of the pulse. As shown in **Figure 11**, the introduction of the EIT effectively suppresses the dissipation of the QB. In this process, the parameter V also affects the ergodicity. Therefore, the dipole–dipole interaction should be minimized as much as possible.

4. Implementation of a Four-Level Quantum Battery

As a concrete example, we propose constructing the QB using the $5S_{1/2}$, $5P_{1/2}$, $5P_{3/2}$, and $6S_{1/2}$ levels of rubidium atoms.[39] First of all, we prepare the rubidium atoms by heating a Rb dispenser to release vapor into the ultra-high-vacuum chamber. We then employ a magneto-optical trap (MOT),[45–47] using counter-propagating σ^+/σ^- cooling beams red-detuned by 10–20 MHz and an anti-Helmholtz coil generating a position-dependent magnetic field gradient, to cool the atoms from thermal velocities down to approximately 100 μK.

Next, a fraction of these cold atoms, on the order of 10^5–10^6, is loaded into a red-detuned optical dipole trap (ODT)[48–50] at 1064 nm. The inhomogeneous intensity profile of the ODT further reduces their temperature to a few microkelvin. By adiabatically transporting the ODT beam via a frequency-shifted optical conveyor, we transfer the atoms into the mode volume of a high-finesse Fabry–Pérot cavity.

Finally, we apply two phase-locked coupling lasers on the Λ-type subsystem formed by the $5P_{1/2}$, $5P_{3/2}$, and $6S_{1/2}$ levels. These

two coherent fields drive the ground state $5S_{1/2}$ into a long-lived dark-state polariton, thereby realizing the desired QB.

5. Conclusion

In summary, we introduce EIT into a four-level atom and transform it into an effectively two-level system consisting of the ground state and the dark state. We then replace the two-level atoms in the QB with these quasi-two-level atoms. Three distinct models are developed: one featuring a single atom and a single photon within a cavity, another with multiple atoms and a single photon, and the third with multiple atoms and multiple photons. We also consider the impact of the dipole–dipole interaction on the ergotropy. Finally, we explore the possibility of using pulses to excite our QB. We investigate the evolution of the QB's energy and ergotropy in these models and find that the introduction of EIT significantly suppresses the decay of both energy and ergotropy compared to scenarios without EIT. Under the specified parameter conditions, the decay rate of the system is reduced by two orders of magnitude upon incorporating EIT. Moreover, by adjusting the coupling frequency ω_c, the ergotropy of the system can be further enhanced. This study demonstrates that the introduction of EIT can significantly extend the lifetime of QBs. Additionally, the energy transfer efficiency during the charging process is improved. These advancements not only enhance the performance of QBs but also pave the way for their broader application in various technological fields.

Appendix A: Diagonization of H_0

In this appendix, we will diagonalize H_0 by the perturbation theory. According to the Schrödinger equation $H|x\rangle = x|x\rangle$, we can obtain the eigen energies x's by the following equation, i.e.,

$$x\left[x^2 - (\omega_1+\omega_2)x + \omega_1\omega_2 - \Omega^2\right] + \Omega_1^2\omega_2 = 0 \tag{A1}$$

where

$$\Omega^2 = \Omega_1^2 + \Omega_2^2 \tag{A2}$$

When ω_2 is small, to the first order of ω_2, the solutions can be written as

$$x_j \simeq x_{0j} + A_j\omega_2 \tag{A3}$$

According to the perturbation theory, the zero-order terms are given by

$$x_{0j}\left[x_{0j}^2 - (\omega_1+\omega_2)x_{0j} + \omega_1\omega_2 - \Omega^2\right] = 0 \tag{A4}$$

where

$$x_{01} = 0 \tag{A5}$$

$$x_{02} = \omega_+ \tag{A6}$$

$$x_{03} = \omega_- \tag{A7}$$

$$\omega_\pm = \frac{1}{2}\left[(\omega_1+\omega_2) \pm \sqrt{(\omega_1-\omega_2)^2 + 4\Omega^2}\right] \tag{A8}$$

After some algebra, we can rewrite Equation (A1) as

$$x(x-\omega_+)(x-\omega_-) + \Omega_1^2\omega_2 = 0 \tag{A9}$$

By substituting $x_1' = A_1\omega_2$ into the above equation, we have

$$A_1\omega_2(A_1\omega_2-\omega_+)(A_1\omega_2-\omega_-) + \Omega_1^2\omega_2 = 0 \tag{A10}$$

Ignoring higher-order terms of ω_2, we can obtain

$$A_1 = -\frac{\Omega_1^2}{\omega_+\omega_-} \simeq \frac{\Omega_1^2}{\Omega^2} \tag{A11}$$

By repeating the above procedure, we have

$$A_2 = -\frac{\Omega_1^2}{\omega_+(\omega_+-\omega_-)} \simeq -\frac{\Omega_1^2}{2\Omega^2} \tag{A12}$$

$$A_3 = \frac{\Omega_1^2}{\omega_-(\omega_+-\omega_-)} \simeq -\frac{\Omega_1^2}{2\Omega^2} \tag{A13}$$

When $\omega_1, \omega_2 \ll \Omega_1, \Omega_2$, to the first-order terms of ω_1 and ω_2, we can obtain

$$\omega_\pm \simeq \frac{1}{2}[(\omega_1+\omega_2) \pm 2\Omega] \tag{A14}$$

In all, the eigen energies are respectively

$$x_1' \simeq \frac{\Omega_1^2}{\Omega^2}\omega_2 \tag{A15}$$

$$x_2 \simeq \Omega + \frac{1}{2}\left(\omega_1 + \frac{\Omega_2^2}{\Omega^2}\omega_2\right) \tag{A16}$$

$$x_3 \simeq -\Omega + \frac{1}{2}\left(\omega_1 + \frac{\Omega_2^2}{\Omega^2}\omega_2\right) \tag{A17}$$

Correspondingly, the eigen states are

$$|E_i\rangle = \frac{1}{N_i}\left\{\left[(x_i-\omega_1)(x_i-\omega_2) - \Omega_2^2\right]|g\rangle\right. \tag{A18}$$

$$\left. + \Omega_1(x_i-\omega_2)|e\rangle + \Omega_1\Omega_2|m\rangle\right\} \tag{A19}$$

where the normalization constants N_i's are given by

$$N_i^2 = \left|(x_i-\omega_1)(x_i-\omega_2) - \Omega_2^2\right|^2 + \left|\Omega_1(x_i-\omega_2)\right|^2 + \left|\Omega_1\Omega_2\right|^2 \tag{A20}$$

To the zero-order terms of ω_1 and ω_2, we have

$$|E_1\rangle \simeq \frac{\Omega_2}{N_1}(-\Omega_2|d\rangle + \Omega_1|m\rangle) \tag{A21}$$

$$|E_2\rangle \simeq \frac{\Omega_1}{N_2}(\Omega_1|d\rangle + \Omega|e\rangle + \Omega_2|m\rangle) \tag{A22}$$

$$|E_3\rangle \simeq \frac{\Omega_1}{N_3}(\Omega_1|d\rangle - \Omega|e\rangle + \Omega_2|m\rangle) \tag{A23}$$

where $|E_1\rangle$ is the dark state because it is a superposition of $|d\rangle$ and $|m\rangle$. The other two eigen states $|E_2\rangle$ and $|E_3\rangle$ are referred to as the bright states, because in addition to $|m\rangle$ they also contain $|e\rangle$, which suffers more from decoherence. The decoherence will cause the aging of the QB. Therefore, we introduce $|E_1\rangle$ to the QB in order to suppress the decoherence.

Appendix B: Reduced Density Matrix of QB

In this appendix, we derive the maximum extractable energy. According to Equations (19)–(20), $|\psi_n^+\rangle$ and $|\psi_n^-\rangle$ can be written in terms of the basis $|n\rangle|E_1\rangle$ and $|n+1\rangle|g\rangle$ as

$$|\psi_n^{\pm}\rangle = \begin{pmatrix} c_{\pm} \\ d_{\pm} \end{pmatrix} \tag{B1}$$

where

$$c_{\pm} = \frac{J}{\sqrt{\left(x_1' + n\omega - \lambda_n^{\pm}\right)^2 + J^2}} \tag{B2}$$

$$d_{\pm} = \frac{\lambda_n^{\pm} - x_1' - n\omega}{\sqrt{\left(x_1' + n\omega - \lambda_n^{\pm}\right)^2 + J^2}} \tag{B3}$$

In the basis $|n\rangle|E_1\rangle$ and $|n+1\rangle|g\rangle$, the time-evolution operator

$$U(t) = e^{-iHt} = \sum_{\alpha=\pm} e^{-i\lambda_n^{\alpha}t}|\psi_n^{\alpha}\rangle\langle\psi_n^{\alpha}| \tag{B4}$$

can be rewritten as

$$U'(t) = PU(t)P^{-1} = \begin{pmatrix} \frac{c_-d_+e^{-i\lambda_n^-t} - c_+d_-e^{-i\lambda_n^+t}}{c_-d_+ - c_+d_-} & \frac{c_+c_-(e^{-i\lambda_n^+t} - e^{-i\lambda_n^-t})}{c_-d_+ - c_+d_-} \\ \frac{d_+d_-(e^{-i\lambda_n^-t} - e^{-i\lambda_n^+t})}{c_-d_+ - c_+d_-} & \frac{c_-d_+e^{-i\lambda_n^+t} - c_+d_-e^{-i\lambda_n^-t}}{c_-d_+ - c_+d_-} \end{pmatrix} \tag{B5}$$

where

$$P = \begin{pmatrix} c_+ & c_- \\ d_+ & d_- \end{pmatrix} \tag{B6}$$

Initially, the system is in the state $|\psi_0\rangle = \alpha|n\rangle|E_1\rangle + \beta|n+1\rangle|g\rangle$. The density matrix $\rho(t) = U'(t)\rho(0)U'^{\dagger}(t)$ at time t reads

$$\rho(t) = \frac{1}{|c_2d_1 - c_1d_2|^2}\begin{pmatrix} M_{11} & M_{12} \\ M_{21} & M_{22} \end{pmatrix} \tag{B7}$$

where

$$\begin{aligned} M_{11} = {} & \left(c_+^*d_-^*e^{i\lambda_n^+t} - c_-^*d_+^*e^{i\lambda_n^-t}\right) \\ & \times \left[(c_+d_-e^{-i\lambda_n^+t} - c_-d_+e^{-i\lambda_n^-t})|\alpha|^2 + c_+c_-(e^{-i\lambda_n^+t} - e^{-i\lambda_n^-t})\beta\alpha^*\right] \\ & + c_+^*c_-^*(e^{i\lambda_n^+t} - e^{i\lambda_n^-t}) \\ & \times \left[c_+c_-(e^{-i\lambda_n^+t} - e^{-i\lambda_n^-t})|\beta|^2 + (-c_+d_-e^{-i\lambda_n^+t} + c_-d_+e^{-i\lambda_n^-t})\alpha\beta^*\right] \end{aligned} \tag{B8}$$

$$\begin{aligned} M_{12} = {} & d_+^*d_-^*(e^{i\lambda_n^+t} - e^{i\lambda_n^-t}) \\ & \times \left[(c_+d_-e^{-i\lambda_n^+t} - c_-d_+e^{-i\lambda_n^-t})|\alpha|^2 + c_+c_-(e^{-i\lambda_n^+t} - e^{-i\lambda_n^-t})\beta\alpha^*\right] \\ & + \left(c_-^*d_+^*e^{i\lambda_n^+t} - c_+^*d_-^*e^{i\lambda_n^-t}\right) \\ & \times \left[c_+c_-(e^{-i\lambda_n^+t} - e^{-i\lambda_n^-t})|\beta|^2 + (-c_+d_-e^{-i\lambda_n^+t} + c_-d_+e^{-i\lambda_n^-t})\alpha\beta^*\right], \end{aligned} \tag{B9}$$

$$\begin{aligned} M_{21} = {} & \left(c_+^*d_-^*e^{i\lambda_n^+t} - c_-^*d_+^*e^{i\lambda_n^-t}\right) \\ & \times \left[d_+d_-(e^{-i\lambda_n^+t} - e^{-i\lambda_n^-t})|\alpha|^2 + (-c_-d_+e^{-i\lambda_n^+t} + c_+d_-e^{-i\lambda_n^-t})\beta\alpha^*\right] \\ & + c_+^*c_-^*(e^{i\lambda_n^+t} - e^{i\lambda_n^-t}) \\ & \times \left[(c_-d_+e^{-i\lambda_n^+t} - c_+d_-e^{-i\lambda_n^-t})|\beta|^2 + d_+d_-(-e^{-i\lambda_n^+t} + e^{-i\lambda_n^-t})\alpha\beta^*\right], \end{aligned} \tag{B10}$$

$$\begin{aligned} M_{22} = {} & d_+^*d_-^*(e^{i\lambda_n^+t} - e^{i\lambda_n^-t}) \\ & \times \left[d_+d_-(e^{-i\lambda_n^+t} - e^{-i\lambda_n^-t})|\alpha|^2 + (-c_-d_+e^{-i\lambda_n^+t} + c_+d_-e^{-i\lambda_n^-t})\beta\alpha^*\right] \\ & + \left(c_-^*d_+^*e^{i\lambda_n^+t} - c_+^*d_-^*e^{i\lambda_n^-t}\right) \\ & \times \left[(c_-d_+e^{-i\lambda_n^+t} - c_+d_-e^{-i\lambda_n^-t})|\beta|^2 + d_+d_-(-e^{-i\lambda_n^+t} + e^{-i\lambda_n^-t})\alpha\beta^*\right]. \end{aligned} \tag{B11}$$

Thus, the reduced density matrix of the QB is

$$\rho_B(t) = \frac{1}{|c_2d_1 - c_1d_2|^2}\begin{pmatrix} M_{11} & 0 \\ 0 & M_{22} \end{pmatrix} \tag{B12}$$

By substituting the above equation into $W(t) = \mathrm{Tr}[\rho_B(t)H_B] - \mathrm{Tr}[\tilde{\rho}_B(t)H_B]$, we can obtain the time evolution of the system's ergodicity.

Appendix C: Time Evolution by Wei-Norman Algebra

In this appendix, we will unravel the time evolution by Wei-Norman algebra.

Since

$$[ab^{\dagger}, b^{\dagger}b - a^{\dagger}a] = -2ab^{\dagger} \tag{C1}$$

$$[a^{\dagger}b, b^{\dagger}b - a^{\dagger}a] = 2a^{\dagger}b \tag{C2}$$

$$[ab^{\dagger}, a^{\dagger}b] = b^{\dagger}b - a^{\dagger}a \tag{C3}$$

the set of operators $\{ab^{\dagger}, a^{\dagger}b, b^{\dagger}b - a^{\dagger}a\} = \{H_1, H_2, H_3\}$ forms a complete set. In order to solve the time-evolution operator $U(t) = \exp(-iHt)$, we can use the Wei-Norman algebra.[41,42] The Hamiltonian H can be rewritten in terms of the above operators as $H = f_1H_1 + f_2H_2 + f_3H_3$. Thus, the time-evolution operator in the interaction picture can be given as the product of a series of exponential operators, i.e.,

$$U_I(t) = \prod_{j=1}^{3} \exp[g_j(t)H_j] \tag{C4}$$

where $g_i(t)$ is a function of time and H_i's are the generators of the Wei-Norman algebra. In the interaction picture, the time-evolution operator is determined by

$$i\frac{dU_I(t)}{dt} = H_IU_I(t) \tag{C5}$$

By substituting Equation (C4) into the above equation, we have

$$\begin{aligned} H_I = {} & i(\dot{g}_1H_1 + e^{g_1H_1}\dot{g}_2H_2e^{-g_1H_1} \\ & + e^{g_1H_1}e^{g_2H_2}\dot{g}_3H_3e^{-g_2H_2}e^{-g_1H_1}) \end{aligned} \tag{C6}$$

Using the Baker-Campbell-Hausdorff formula,[43] we can obtain

$$e^{g_1 H_1} \dot{g}_2 H_2 e^{-g_1 H_1} = \dot{g}_2[a^\dagger b + g_1(b^\dagger b - a^\dagger a) - g_1^2 a b^\dagger] \tag{C7}$$

By repeating the above procedure, we have

$$\dot{g}_3[2g_2 a^\dagger b - (2g_1 + 2g_1^2 g_2) a b^\dagger + (1 + 2g_1 g_2)(b^\dagger b - a^\dagger a)]$$
$$= e^{g_1 H_1} e^{g_2 H_2} \dot{g}_3 H_3 e^{-g_2 H_2} e^{-g_1 H_1} \tag{C8}$$

By substituting Equations (C7) and (C8) into H_I, we can obtain

$$\begin{aligned} H_I = i\{&(\dot{g}_2 + 2\dot{g}_3 g_2) a^\dagger b \\ &+ [\dot{g}_1 - \dot{g}_2 g_1^2 - \dot{g}_3(2g_1 + 2g_1^2 g_2)] a b^\dagger \\ &+ [\dot{g}_2 g_1 + \dot{g}_3(1 + 2g_1 g_2)](b^\dagger b - a^\dagger a)\} \end{aligned} \tag{C9}$$

By comparing the above equation with $H_I = J\sqrt{N}(a b^\dagger + a^\dagger b)$, we have

$$\dot{g}_1 - \dot{g}_2 g_1^2 - \dot{g}_3(2g_1 + 2g_1^2 g_2) = -iJ_N \tag{C10}$$

$$\dot{g}_2 + 2\dot{g}_3 g_2 = -iJ_N \tag{C11}$$

$$\dot{g}_2 g_1 + \dot{g}_3(1 + 2g_1 g_2) = 0 \tag{C12}$$

Assuming the initial condition $g_1(0) = g_2(0) = g_3(0) = 0$, we can obtain

$$g_1 = -i\tan(J_N t) \tag{C13}$$

$$g_2 = -\frac{i}{2}\sin(2J_N t) \tag{C14}$$

$$g_3 = -\ln[\cos(J_N t)] \tag{C15}$$

Therefore, the time-evolution operator reads

$$U(t) = U_0(t) U_I(t) \tag{C16}$$

$$U_0(t) = \exp\left[-i\omega_0 t(a^\dagger a + b^\dagger b)\right] \tag{C17}$$

$$U_I(t) = e^{g_1 a b^\dagger} e^{g_2 a^\dagger b} e^{g_3(b^\dagger b - a^\dagger a)} \tag{C18}$$

Acknowledgements

This work was supported by the Innovation Program for Quantum Science and Technology under Grant No. 2023ZD0300200, the National Natural Science Foundation of China under Grant No. 62461160263, the Beijing Natural Science Foundation under Grant No. 1202017, and the Beijing Normal University under Grant No. 2022129.

Conflict of Interest

The authors declare no conflict of interest.

Data Availability Statement

The data that support the findings of this study are available from the corresponding author upon reasonable request.

Keywords

dark states, electromagnetically-induced, quantum batteries

Received: June 30, 2025
Published online:

[1] R. A. Dunlap, O. Mao, J. R. Dahn, *Phys. Rev. B* **1999**, *59*, 3494.
[2] A. H. Castro Neto, F. Guinea, N. M. R. Peres, K. S. Novoselov, A. K. Geim, *Rev. Mod. Phys.* **2009**, *81*, 109.
[3] P. Parmananda, P. Sherard, R. W. Rollins, H. D. Dewald, *Phys. Rev. E* **1993**, *47*, R3003.
[4] F. Campaioli, F. A. Pollock, S. Vinjanampathy, *Thermodynamics in the Quantum Regime: Fundamental Aspects and New Directions*, (Eds.: F. Binder, L. A. Correa, C. Gogolin, J. Anders, G. Adesso), Springer, Switzerland **2018**.
[5] , K. Tordrup, A. Negretti, K. Mølmer, *Phys. Rev. Lett.* **2008**, *101*, 040501.
[6] N. Berthusen, D. Devulapalli, E. Schoute, A. M. Childs, M. J. Gullans, A. V. Gorshkov, D. Gottesman, *PRX Quantum* **2025**, *6*, 010306.
[7] L. A. Pettersson, A. S. Sørensen, S. Paesani, *PRX Quantum* **2025**, *6*, 010305.
[8] I. Soloviev, S. Bakurskiy, V. Ruzhickiy, N. Klenov, M. Kupriyanov, A. Golubov, O. Skryabina, V. Stolyarov, *Phys. Rev. Appl.* **2021**, *16*, 044060.
[9] C. A. Vincent, B. Scrosati, *Modern Batteries: An Introduction to Electrochemical Power Sources*, 2nd ed., Butterworth-Heinemann, UK **1997**.
[10] L. Labonté, O. Alibart, V. D'Auria, F. Doutre, J. Etesse, G. Sauder, A. Martin, E. Picholle, S. Tanzilli, *PRX Quantum* **2024**, *5*, 010101.
[11] W.-L. Song, H.-B. Liu, B. Zhou, W.-L. Yang, J.-H. An, *Phys. Rev. Lett.* **2024**, *132*, 090401.
[12] F. H. Kamin, F. T. Tabesh, S. Salimi, A. C. Santos, *Phys. Rev. E* **2020**, *102*, 052109.
[13] T. P. Le, J. Levinsen, K. Modi, M. M. Parish, F. A. Pollock, *Phys. Rev. A* **2018**, *97*, 022106.
[14] S. Deffner, S. Campbell, *Quantum Thermodynamics: An Introduction to the Thermodynamics of Quantum Information*, Iop Concise Physics Publishing, UK **2019**.
[15] D. Mayer, E. Lutz, A. Widera, *Commun. Phys.* **2023**, *6*, 61.
[16] G. Maslennikov, S. Ding, R. Hablützel, J. Gan, A. Roulet, S. Nimmrichter, J. Dai, V. Scarani, D. Matsukevich, *Nat. Commun.* **2019**, *10*, 202.
[17] J. Zhou, A. Li, M. Galperin, *Phys. Rev. B* **2024**, *109*, 085408.
[18] M. L. Bera, T. Pandit, K. Chatterjee, V. Singh, M. Lewenstein, U. Bhattacharya, M. N. Bera, *Phys. Rev. Res.* **2024**, *6*, 013318.
[19] F. Campaioli, S. Gherardini, J. Q. Quach, M. Polini, G. M. Andolina, *Rev. Mod. Phys.* **2024**, *96*, 031001.
[20] S. Bhattacharjee, A. Dutta, *Eur. Phys. J. B* **2021**, *94*, 239.
[21] R. Alicki, M. Fannes, *Phys. Rev. E* **2013**, *87*, 042123.
[22] D. Ferraro, M. Campisi, G. M. Andolina, V. Pellegrini, M. Polini, *Phys. Rev. Lett.* **2018**, *120*, 117702.
[23] G. M. Andolina, M. Keck, A. Mari, M. Campisi, V. Giovannetti, M. Polini, *Phys. Rev. Lett.* **2019**, *122*, 047702.
[24] F. Pirmoradian, K. Mølmer, *Phys. Rev. A* **2019**, *100*, 043833.
[25] A. Crescente, M. Carrega, M. Sassetti, D. Ferraro, *Phys. Rev. B* **2020**, *102*, 245407.
[26] W.-X. Guo, F.-M. Yang, F.-Q. Dou, *Phys. Rev. A* **2024**, *109*, 032201.
[27] K. Xu, H.-G. Li, Z.-G. Li, H.-J. Zhu, G.-F. Zhang, W.-M. Liu, *Phys. Rev. A* **2022**, *106*, 012425.
[28] Y. Yao, X. Q. Shao, *Phys. Rev. E* **2022**, *106*, 014138.
[29] S.-Y. Bai, J.-H. An, *Phys. Rev. A* **2020**, *102*, 060201(R).
[30] M. Fleischhauer, A. Imamoglu, J. P. Marangos, *Rev. Mod. Phys.* **2005**, *77*, 633.
[31] K.-J. Boller, A. Imamoğlu, S. E. Harris, *Phys. Rev. Lett.* **1991**, *66*, 2593.
[32] S. E. Harris, J. E. Field, A. Imamoğlu, *Phys. Rev. Lett.* **1990**, *64*, 1107.
[33] E. Paspalakis, P. L. Knight, *Phys. Rev. A* **2001**, *63*, 065802.
[34] Y.-Y. Wang, J. Qiu, Y.-Q. Chu, M. Zhang, J. Cai, Q. Ai, F.-G. Deng, *Phys. Rev. A* **2018**, *97*, 042313.
[35] M. Fleischhauer, M. D. Lukin, *Phys. Rev. Lett.* **2000**, *84*, 5094.
[36] M. D. Reed, L. DiCarlo, B. R. Johnson, L. Sun, D. I. Schuster, L. Frunzio, R. J. Schoelkopf, *Phys. Rev. Lett.* **2010**, *105*, 173601.
[37] J. Q. Quach, W. J. Munro, *Phys. Rev. Appl.* **2020**, *14*, 024092.

[38] A. C. Santos, B. Çakmak, S. Campbell, N. T. Zinner, *Phys. Rev. E* **2019**, *100*, 032107.
[39] O. Jitrik, C. F. Bunge, *J. Phys. Chem. Ref. Data* **2005**, *33*, 1059.
[40] T. Holstein, H. Primakoff, *Phys. Rev.* **1940**, *58*, 1098.
[41] J. Wei, E. Norman, *J. Math. Phys.* **1963**, *4*, 575.
[42] D. Z. Xu, Q. Ai, C. P. Sun, *Phys. Rev. A* **2011**, *83*, 022107.
[43] J. Sakurai, J. Napolitano, *Modern Quantum Mechanics*, 2nd ed., Addison-Wesley, San Francisco **2011**.
[44] Z. Ficek, R. Tanaś, *Phys. Rep.* **2002**, *372*, 369.
[45] Z. Zeng, S. Deng, S. Yang, B. Yan, *Phys. Rev. Lett.* **2024**, *133*, 143404.
[46] M. Gaudesius, Y.-C. Zhang, T. Pohl, R. Kaiser, G. Labeyrie, *Phys. Rev. A* **2022**, *105*, 013112.
[47] J. Schoser, A. Batär, R. Löw, V. Schweikhard, A. Grabowski, Y. B. Ovchinnikov, T. Pfau, *Phys. Rev. A* **2002**, *66*, 023410.
[48] D. Frese, B. Ueberholz, S. Kuhr, W. Alt, D. Schrader, V. Gomer, D. Meschede, *Phys. Rev. Lett.* **2000**, *85*, 3777.
[49] J. J. Zirbel, K.-K. Ni, S. Ospelkaus, T. L. Nicholson, M. L. Olsen, P. S. Julienne, C. E. Wieman, J. Ye, D. S. Jin, *Phys. Rev. A* **2008**, *78*, 013416.
[50] H. J. Lee, C. S. Adams, M. Kasevich, S. Chu, *Phys. Rev. Lett.* **1996**, *76*, 2658.